DOI:10.11817/j.issn.1672-7347.2024.230308

Transcriptomic analysis reveals “adipogenesis” in the uterosacral ligaments of postmenopausal women with recurrent pelvic organ prolapse

ZHOU Yanhua[1], YAN Dayu[2], ZHANG Xiulan[1], LI Xuhong[1], YAN Wenguang[1], JIANG Li[1,3]

(1. Department of Rehabilitation Medicine, Third Xiangya Hospital, Central South University, Changsha 410013;
2. Department of Obstetrics and Gynecology, Third Xiangya Hospital, Central South University, Changsha 410013;
3. Postdoctoral Research Station of Basic Medicine, Third Xiangya Hospital, Central South University, Changsha 410013, China)

ABSTRACT

Objective: Pelvic organ prolapse (POP) is a common condition in postmenopausal women, with an increasing prevalence due to aging. Some women experience POP recurrence after surgical treatment, significantly affecting their physical and mental health. The uterosacral ligament is a critical pelvic support structure. This study aims to investigate the molecular pathological changes in the uterosacral ligament of postmenopausal women with recurrent POP using transcriptomic analysis.

Methods: Transcriptomic data of uterosacral ligament tissues were obtained from the public dataset GSE28660, which includes samples from 4 postmenopausal women with recurrent POP, 4 with primary POP, and 4 without POP. Differentially expressed genes (DEGs) were identified between recurrent POP and both primary and non-POP groups. Further analysis included intersection analysis of DEGs, gene ontology enrichment, protein-protein interaction (PPI) network construction, gene set enrichment analysis (GSEA), single-sample GSEA, and xCell immune cell infiltration analysis to explore molecular pathological changes in recurrent POP. Additionally, histological and molecular differences in the uterosacral ligament were compared between simulated vaginal delivery (SVD) rat models with and without ovariectomy.

Results: Compared with primary POP and non-POP groups, recurrent POP exhibited activation of adipogenesis and inflammation-related pathways, while pathways related to muscle proliferation and contraction were downregulated in the uterosacral ligament. Nine

Date of reception: 2023-08-12

First author: ZHOU Yanhua, Email: 42351847@qq.com, ORCID: 0000-0002-8640-1934; YAN Dayu, Email: yandayu123@163.com, ORCID: 0009-0004-7417-1109

Corresponding author: JIANG Li, Email: csujiangli@163.com, ORCID: 0000-0002-4422-567X

Foundation item: This work was supported by the Key Research and Development Program of Hunan Province (2023SK2038) and the Natural Science Foundation of Hunan Province (2024JJ8121), China.

key DEGs (*ADIPOQ, FABP4, IL-6, LIPE, LPL, PCK1, PLIN1, PPARG,* and *CD36*) were identified, with most enriched in the peroxisome proliferator-activated receptor (PPAR) signaling pathway. These genes were significantly correlated with lipid accumulation, monocyte infiltration, and neutrophil infiltration in the uterosacral ligament. Urodynamic testing revealed that the bladder leak point pressure was significantly higher in ovariectomized SVD rats, both of which had higher values than the sham group. Masson staining showed pronounced adipogenesis in the uterosacral ligament of ovariectomized SVD rats, along with reduced collagen and muscle fibers compared to the sham and non-ovariectomized SVD groups. Furthermore, real-time RT-PCR confirmed significantly elevated expression of key DEGs, including *ADIPOQ, IL-6, PCK1,* and *PLIN1*, in the uterosacral ligaments of ovariectomized SVD rats.

Conclusion: Adipogenesis and inflammation in the uterosacral ligament may contribute to its reduced supportive function, potentially leading to recurrence POP in postmenopausal women.

KEY WORDS recurrent pelvic organ prolapse; uterosacral ligament; adipogenesis; inflammation; transcriptomics

转录组学分析揭示复发性盆腔器官脱垂的绝经后妇女存在子宫骶韧带“脂肪化”

周艳华[1]，严大宇[2]，张秀兰[1]，李旭红[1]，严文广[1]，姜丽[1,3]

(1. 中南大学湘雅三医院康复医学科，长沙 410013；2. 中南大学湘雅三医院妇产科，长沙 410013；
3. 中南大学湘雅三医院基础医学博士后工作站，长沙 410013)

[摘 要] 目的： 盆腔器官脱垂(pelvic organ prolapse，POP)是绝经后妇女的常见病，随着老龄化时代的到来，其发病率呈逐年上升趋势。部分POP妇女在手术治疗后仍有复发现象，严重影响其身心健康。子宫骶韧带是盆底的重要支持结构之一。本研究拟通过转录组学分析揭示子宫骶韧带在绝经后复发性POP中的分子病理变化。**方法：** 收集公共数据集GSE28660(包含4名绝经后复发性POP、4名原发性POP和4名非POP妇女)中子宫骶韧带的转录组数据，分别计算复发性POP与原发性POP或非POP的差异表达基因。随后，通过差异基因交集分析、基因本体论、蛋白质-蛋白质互作网络构建、基因集富集分析、单样本基因集富集分析以及xCell免疫细胞浸润分析等方法分析复发性POP中子宫骶韧带的分子病理变化。比较卵巢切除和未切除的模拟阴道分娩(simulated vaginal delivery，SVD)大鼠模型的子宫骶韧带的病理结构和分子表达的变化。**结果：** 相比于原发性POP和非POP，复发性POP的子宫骶韧带中脂肪和炎症相关的通路被激活，而与肌肉增殖和收缩相关的通路被抑制。鉴定出的9个关键差异基因(*ADIPOQ*、*FABP4*、*IL-6*、*LIPE*、*LPL*、*PCK1*、*PLIN1*、*PPARG* 和 *CD36*)，大部分富集在过氧化物酶体增殖激活受体(peroxisome proliferator activated receptor，PPAR)信号通路中，且与子宫骶韧带中的脂肪细胞堆积、单核细胞和中性粒细胞浸润呈显著正相关。尿动力学检测显示卵巢切除SVD大鼠的膀胱漏尿点压力明显高于卵巢未切除SVD大鼠，这2组大鼠的膀胱漏尿点压力均高于假手术组。马松染色结果显示：相比于假手术组和卵巢未切除SVD大鼠，卵巢切除SVD大鼠的子宫骶韧带存在明显的脂肪堆积，胶原纤维和肌纤维成分减少。此外，实时反转录PCR也验证了关键差异基因 *ADIPOQ*、*IL-6*、*PCK1*、*PLIN1* 均在卵巢切除SVD大鼠的子宫骶韧带中呈显著高表达。**结论：** 子宫骶韧带出现脂肪堆积并伴发炎症从而导致其支持功能下降，可能是绝经后妇女发生复发性POP的原因之一。

[关键词] 复发性盆腔器官脱垂；子宫骶韧带；脂肪化；炎症；转录组学

Pelvic organ prolapse (POP) is defined by a descending or drooping of any pelvic apparatus and/or vaginal compartments, involving a diversity of urinary, rectum, or bowel, gynecological, and sexual

manifestations[1]. It is a prevalent condition affecting millions of women worldwide. Surgery is one of the main treatments for POP, and the lifetime risk of surgery for POP in the female population is 13% to 19%[2]. However, recurrent POP is not uncommon, which means the previous surgery failed, regardless of whether it was subjective and/or objective[3]. Also, the medical cost for a POP surgery is considerable in many countries, as such, recurrent POP further increases the economic burden, especially in the era of global aging[4].

Nevertheless, the etiology of recurrent POP is complex and largely unknown, which is probably attributed to 2 primary categories: Patient-related factors and procedure-related factors[5]. Assuming the medical treatment procedure is relatively standardized, patient-related factors seem to account for a higher risk for POP recurrence[3]. As is known, the deficiency of the supportive and/or connective tissue is considered as contributing to the development of POP[1]. For example, the prolapse of the anterior vaginal compartment, likely the most common form of recurrent POP, is considered strongly related to apical support defects[6]. And the apex support reconstruction significantly reduces the risk for POP recurrence[7]. The apical support system is composed mainly of the cardinal and uterosacral ligaments[8]. Noticeably, the uterosacral ligaments are usually employed as a supportive anchors in POP reconstructive surgery, and surgery without uterosacral ligament suspension might be linked to the surgical failures or recurrence of various compartments prolapses[9-10]. Studies[11-12] at the molecular level suggested significant alterations related to connective tissue collagen formation and inflammatory cell infiltration in the uterosacral ligament of POP compared to healthy controls. However, the molecular changes of the uterosacral ligaments in recurrent POP patients remain poorly explored.

With a tremendous upsurge of transcriptomic technology in the past few years, including the advanced sequencing and microarray detecting technique, it is feasible now to examine the pathogenesis of diseases at a more subtle perspective and high-throughput level. In this study, we aim to analyze the molecular changes in uterosacral ligaments from women with recurrent POP compared to those from non-POP and primary-POP women using publicly available datasets. Additionally, we aim to validate the effect of estrogen deficiency on the structural changes in the uterosacral ligament using non-ovariectomized and ovariectomized simulated vaginal delivery (SVD) rat models.

1 Materials and methods

1.1 Data mining and preprocessing

We performed a data search with the keywords “recurrent pelvic organ prolapse” “recurrent prolapse” or “recurrent POP” in the Gene Expression Omnibus database repository (GEO). We only found one suitable microarray dataset, GSE28660, which profiled the gene expression of uterosacral ligaments from 4 postmenopausal women with recurrent-POP, 4 with primary-POP, and 4 without POP. Patient’s information is summarized in Supplementary Table 1 (https://doi.org/10.57760/sciencedb.xbyxb.00021).

The GSE28660 microarray dataset was based on the platform GPL2895 (GE Healthcare/Amersham Biosciences CodeLink Human Whole Genome Bioarray). All data preprocessing was performed in Rstudio software by using the R language. Firstly, the gene expression matrix and annotation file of GSE28660 was downloaded by R package “GEOquery”. Then, the expression matrix was normalized by quantile and $\log_2$ function. Moreover, the probes were matched to gene symbols according to the annotation file. Principal component analysis (PCA) was performed to examine distribution of samples and determine the contrast matrices.

1.2 Identification of differentially expressed genes

After data preprocessing, differentially expressed genes (DEGs) in each contrast matrix were calculated by R package “LIMMA”[13], and screened by a threshold set at a P<0.01 and a $|\log_2$ fold change (FC)|>1. Volcano plots and heatmaps were drawn to visualize the distribution of DEGs. Furthermore, shared DEGs were intersected between different contrast matrixes.

1.3 Functional annotations of DEGs

Gene Ontology (GO) analysis generally includes 3 categories: Biological processes (BPs), cellular components (CCs), and molecular functions (MFs) [14].

The Kyoto Encyclopedia of Genes and Genomes (KEGG) database provides manually collected pathways mapped by various entities, such as genes, proteins, and chemical compounds[15]. Herein, we searched for functional remarks within the GO and KEGG pathways at the website Enrichr, an efficient online tool integrating multiple databases for gene functional annotation. Enriched results with a $P<0.05$ were considered statistically significant. The software Cytoscape was employed to visualize the relationship between enriched pathways and corresponding genes.

1.4 Construction of protein-protein interaction networks

The shared DEGs were uploaded to the Search Tool for the Retrieval of Interacting Genes (STRING) database to predict plausible protein-protein interaction networks, which might provide insights into the pathogenesis of diseases at the protein level. A threshold of interaction score >0.4 was selected. Then, the protein-protein interaction (PPI) network was imported to the software Cytoscape for visualization. Additionally, the plugin MCODE was used to filter hub genes in the PPI network.

1.5 Gene set enrichment analysis and single sample gene set enrichment analyses

Gene Set Enrichment Analysis (GSEA) is a popular algorithm that evaluates whether well-defined pathways show statistically significant differences between 2 biological groups without the requirement of a threshold screening of DEGs[16]. Therefore, we adopted the R package "Clusterprofiler" to perform GSEA analysis between each contrast matrix, and the "c2.cp.kegg.v7.2.symbols. gmt" file was downloaded from GSEA websites as a background gene set. The results with a $P<0.05$ and a $q<0.05$ were considered significantly different.

The single-sample gene set enrichment (ssGSEA) method, an extensive application of GSEA, makes calculating the enrichment score of pre-defined pathways or gene sets in each sample possible[16]. Herein, the ssGSEA was carryout by R package "GSVA" with referring the same gene set "c2.cp.kegg.v7.2.symbols.gmt"[17]. Then, the ssGSEA scores for each pathway were compared between the control (i. e. without POP) and the experiment samples using the R package "LIMMA", and a criterion for a $P<0.01$ was set to select differentially enriched pathways. The correlation of pathways was analyzed by the Spearman method, and a $P<0.05$ was considered statistically significant.

1.6 Microenvironment analysis for uterosacral ligaments

The cellular composition of the microenvironment reflects the milieu of tissues, which opens a more nuanced perspective for us to understand the biological changes in the tissues. The xCell method allows applying expression profiles to calculate the enrichment score of multiple cell types, including immune and non-immune cells, by combining the virtues of gene set enrichment and deconvolution algorithms[18]. Hence, we employed the xCell method in R software for dissecting the enrichment of specific cell types in control and POP uterosacral ligaments. "Kruskal. test" in R package "ggpubr" was applied for comparing the 3 groups' enrichment score, and a $P<0.05$ was considered as significant. Furthermore, the Spearman analysis was used to evaluate the correlation between differentially enriched cell types and hub genes.

1.7 Establishment of simulated vaginal delivery rat models

Since childbirth is one of the most important triggers of pelvic floor dysfunction disorders, such as POP and stress urinary incontinence (SUI), we used the classical vaginal balloon dilatation method to establish the simulated vaginal delivery (SVD) rat model. The usage and operation of all rats were certified by the Ethics Committee of the Department of Laboratory Animals of Central South University (Ethics No: CSU-2023-0296).

Female specific pathogen free (SPF) Sprague-Dawley rats aged 8 weeks and weighing 280 – 330 g were randomly assigned to 3 groups: A sham group, a non-ovariectomized SVD group, and an ovariectomized SVD group. All rats were housed in a controlled environment with a temperature of (22±2) ℃, humidity of (50±10)%, and a 12 h light/dark cycle. The rats were provided with ad libitum access to standard rodent chow and water, and were allowed a one-week acclimatization

period before the start of the experiment to ensure their health and well-being. During this period, their weights were monitored daily to ensure stability. All rats were operated under urethane anesthesia. In the non-ovariectomized SVD group, a balloon catheter was inserted into the rat vagina and secured, and the balloon was perfused with 5 mL of sterile saline to create vertical traction (weighing approximately 0.3 kg), lasting for 8 h. For the ovariectomized SVD group, after completion of the initial SVD modeling, an incision was made on each side of their back, the ovaries were located by layer wise dissection and excised, and then the incision was finally sutured. For rats in the sham group, catheter was inserted into the vagina without balloon saline insufflation.

Because the direction of gravity is differs between rats and humans, vaginal stretching does not result in significant organ prolapse. However, it may induce urodynamic changes resembling SUI and muscle and ligament changes similar to POP[19]. Hence, on day 21 after modeling, maximum bladder capacity (MBC), bladder leak-point pressure (BLPP), and abdominal leak point pressure (ALPP) were measured by ALC-CMG intravesical pressure monitor (Alcott Biotech Company, Shanghai, China) following the methodology described in our previous study[20]. And blood was collected for measurement of estrogen levels according to the ELISA kit instructions (E-OSEL-R0001, Elabscience, China). Finally, all rats were euthanized and dissected to obtain uterosacral ligaments for fixation in 4% paraformaldehyde for subsequent testing.

1.8 Masson staining

Masson staining of the uterosacral ligaments of rats after modeling was performed with reference to previous methods[21]. After routine xylene dewaxing and hydration with different gradients of ethanol, paraffin sections were stained with Weigert's iron hematoxylin solution for 8 min. After acidic ethanol differentiation for 15 s, sections were re-blued by Masson's blue staining for 5 min and then washed with distilled water. After Masson ponceau magenta staining for 5 min, sections were washed using a weak acid solution and then treated with 1% phosphomolybdic acid solution for 3 min. Finally, after routine steps of ethanol dehydration and xylene transparency, the slices were sealed using resin and observed under a microscope (Nikon DS-U3 color digital camera, Japan).

1.9 Real-time RT-PCR

Total RNA was extracted from the uterosacral ligaments with reference to the instructions of the RNA-easy Isolation Reagent kit (#R701-01, Vazyme, Nanjing, China), and reverse transcribed into cDNA using Hiscript II Q RT SuperMix for real-time PCR (#R223-01, Vazyme, Nanjing, China). Real-time RT-PCR was then performed using ChamQ Universal SYBR qPCR Master Mix (#Q711-02, Vazyme, Nanjing, China), and β-actin (No. B661202, Sangon Biotech, Shanghai, China) was selected as internal reference. All primers were synthesized by Sangon Biotech (Shanghai, China), and the specific sequences were as follows: *ADIPOQ*, forward 5'-CGCAGGTGTTCTTGGTCCTAAGG-3', reverse 5'-GCCCTACGCTGAATGCTGAGTG-3'; *IL-6*, forward 5'-ACTTCCAGCCAGTTGCCTTCTTG-3', reverse 5'-TGGTCTGTTGTGGGTGGTATCCTC-3'; *PCK1*, forward 5'-GGGTGTTTACTGGGAAGGCATCG-3', reverse 5'-ACGGTTCCTCATCCTGTGGTCTC-3'; *PLIN1*, forward 5'-GACAGACACAGAGGGAGAGGAGAC-3', reverse 5'-CCACCCAGGAAGCCGAGAGG-3'. The reaction procedure consists of 3 main steps: 1) Pre-denaturation (95 ℃ for 30 s); 2) cycling reaction (95 ℃ for 5 s to denature, then 60 ℃ for 30 s to complete 40 cycles); 3) solubility profile analysis (95 ℃ for 15 s, then lowered to 60 ℃ and held for 60 s, and finally raised to 95 ℃ again and held for 15 s).

2 Results

2.1 Data preprocessing and PCA analysis

After normalization, the boxplot showed the distribution of data for each sample was comparable within the same range (Figure 1A). The PCA analysis indicated that both non-POP and primary POP uterosacral ligaments were obviously distinct from those recurrent POP samples (Figure 1B and 1C), while the difference between non-POP and primary POP uterosacral ligaments was not significant (Figure 1B and 1C). Hence, to focus on the molecular change in the recurrent POP uterosacral ligaments, we chose principal components to construct 2 contrast matrices: 1)

Recurrent POP vs primary POP uterosacral ligaments; 2) recurrent POP vs non-POP uterosacral ligaments. Next, the DEGs in these 2 comparative matrices were obtained separately.

2.2 Identification of DEGs

With the threshold of $|\log_2 FC|>1$ and $P<0.01$, the volcano plots showed that there were 539 DEGs (325 upregulated and 214 downregulated genes) identified between recurrent POP and primary POP uterosacral ligaments (Figure 2A), along with 361 DEGs (269 upregulated and 92 downregulated genes) between recurrent POP and non-POP uterosacral ligaments (Figure 2B). The heatmaps also revealed that the DEGs could distinguish uterosacral ligaments of control or primary POP women from those of recurrent POP women (Figure 2C and 2D). Furthermore, we found that 179 shared DEGs were intersected between recurrent POP vs primary POP uterosacral ligaments and recurrent POP vs non-POP uterosacral ligaments (Figure 2E). These 179 shared DEGs presented the same expression trend in each contrast matrix where 148 DEGs were upregulated, and 31 DEGs were downregulated (Figure 2F).

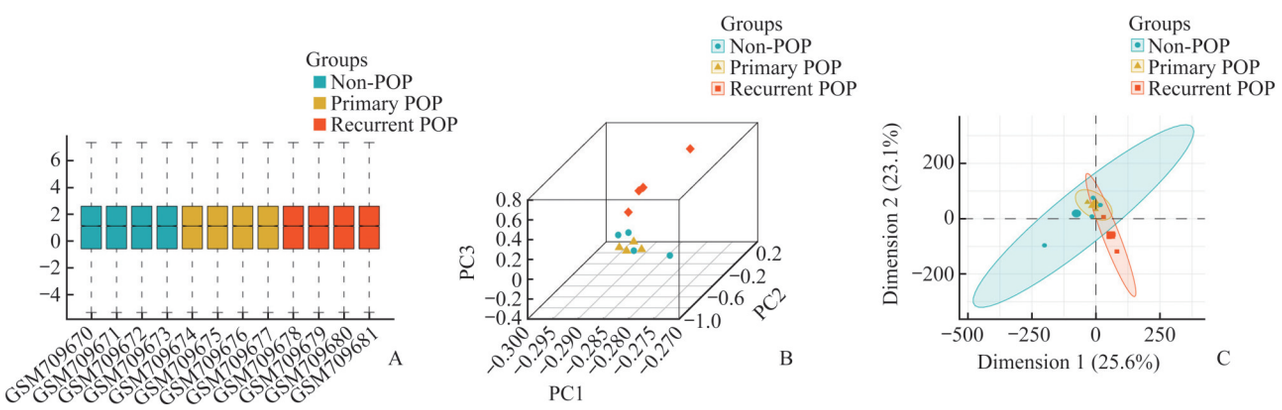

Figure 1 Data preprocessing and PCA analysis

A: Boxplots illustrates the gene expression levels after normalization of the GSE28660 dataset. Boxplots represented the mean and interquartile range. The abscissa axis represents individual samples, and the vertical axis represents gene expression levels. B and C: Three-dimensional (B) and two-dimensional (C) PCA show that both non-POP and primary POP uterosacral ligaments are distinct from those recurrent POP samples. POP: Pelvic organ prolapse; PCA: Principal component analysis; PC: Principal component.

2.3 Functional annotations of shared DEGs

The GO analysis of 179 shared DEGs showed that they were significantly enriched in fat and lipid-associated biological processes (BPs) such as "long-chain fatty acid transport" and "regulation of lipid metabolic process" (Figure 3A), cellular components (CCs) such as "lipid droplet" (Figure 3B), and molecular functions (MFs) such as "steroid dehydrogenase activity" and "fatty acid ligase activity" (Figure 3C). Notably, the significantly enriched "oxidoreductase activity" relevant MFs and CCs such as "mitochondrial outer membrane" and "mitochondrial matrix" probably indicated oxidative phosphorylation were activated in adipose tissues in uterosacral ligaments of recurrent POP women (Figure 3B and 3C). Interestingly, the BP terms "negative regulation of vascular smooth muscle cell proliferation" and "negative regulation of smooth muscle cell proliferation" were also significantly enriched, mainly by 3 DEGs: *IL-10*, *ADIPOQ*, and *PPARG* (data not shown).

Furthermore, the KEGG analysis also indicated that these shared DEGs were significantly enriched in fat and lipid-associated pathways, including "peroxisome proliferator activated receptor (PPAR) signaling pathway" "AMPK signaling pathway" "adipocytokine signaling pathway" "steroid hormone biosynthesis" and "insulin resistance" (Figure 3D). Furthermore, the

"ECM-receptor interaction" was also enriched, probably indicating extracellular matrix alteration in recurrent POP uterosacral ligaments. The top 10 enriched KEGG pathways and corresponding enriched DEGs were used for constructing a pathway-gene network (Figure 3E), in which *CD36* connected to the majority of pathways (Figure 3F).

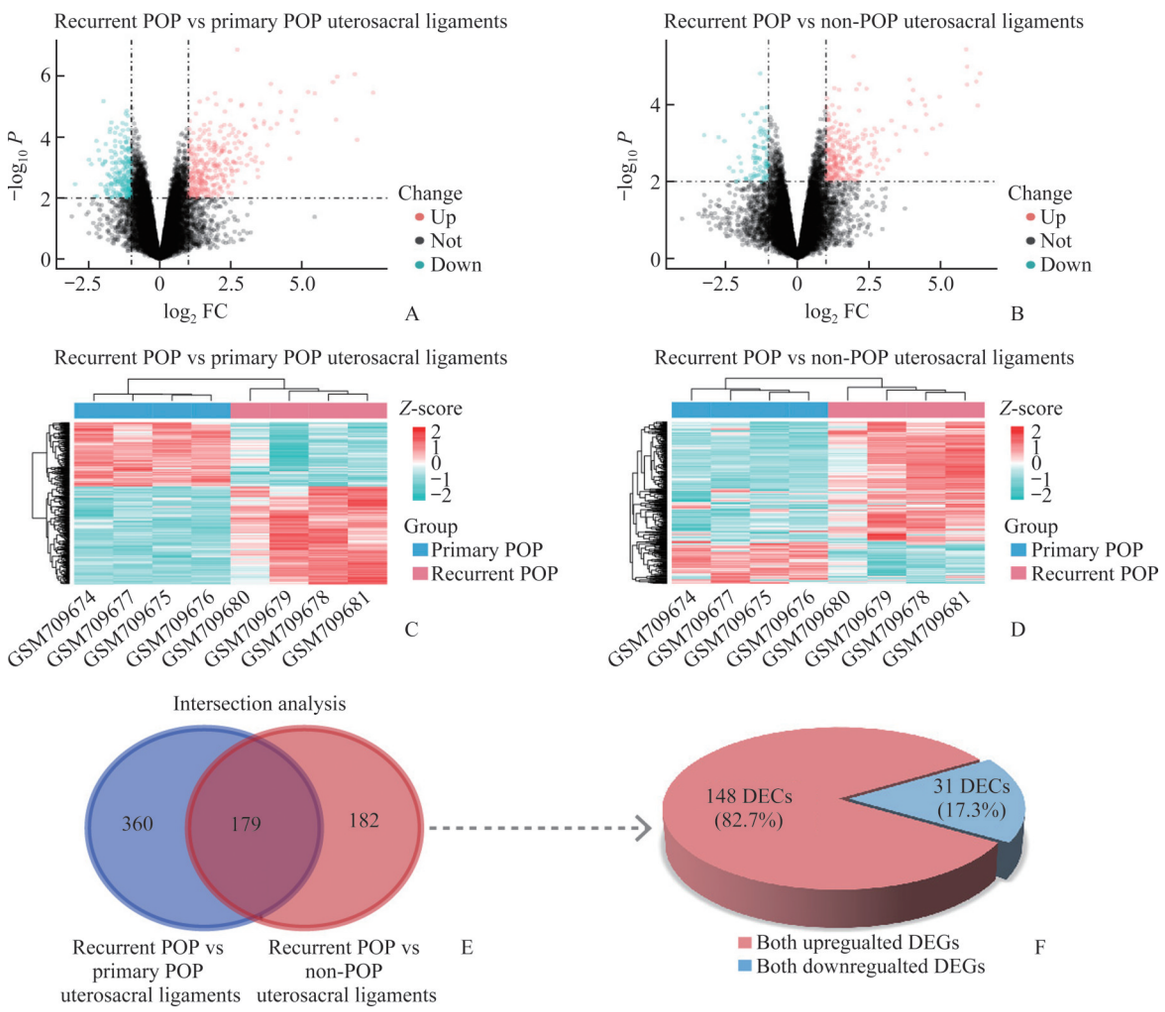

Figure 2 Identification of shared DEGs between recurrent POP and primary POP uterosacral ligaments or recurrent POP and non-POP uterosacral ligaments

A and B: Volcano plots show the distribution of DEGs in the uterosacral ligaments of recurrent POP vs primary POP (A) and recurrent POP vs non-POP uterosacral ligaments (B) in GSE28660. C and D: Heatmap plots display hierarchical clustering of DEGs in the uterosacral ligaments of recurrent POP vs primary POP (C) and recurrent POP vs non-POP uterosacral ligaments (D) in GSE28660. E: Venn diagram shows the shared DEGs ($|\log_2 FC>1|$ and $P<0.05$) between the 2 contrast matrices. F: Pie chart displays the expression trend distribution for the shared DEGs. DEGs: Differentially expressed genes; POP: Pelvic organ prolapse; FC: Fold change.

2.4 PPI network construction

With criteria of interaction score>0.4, a PPI network containing 78 nodes and 224 edges was constructed and then visualized in Cytoscape (Figure 4A). Moreover, with the connective degree calculated by the plugin MOCODE, the top 8 connective nodes identified were *ADIPOQ, FABP4, IL-6, LIPE, LPL, PCK1, PLIN1,* and *PPARG,* forming a core subnetwork (Figure 4B). Hence, these 8 genes and *CD36* (the central connector of the top 10 significantly enriched pathways) were identified as hub genes. Interestingly, most of them were members of the PPAR signaling pathways, such as *ADIPOQ, FABP4, LPL, PCK1, PLIN1,* and *PPARG*.

Figure 3 Functional annotations of shared DEGs between recurrent POP and primary POP uterosacral ligaments or recurrent POP and non-POP uterosacral ligaments

A−D: Horizontal bars represent the top 10 significantly enriched GO terms, including biological processes (A), molecular functions (B), cellular components (C), and KEGG pathways (D) of the shared DEGs. E: A pathway-gene network constructed using Cytoscape software for the top 10 enriched KEGG pathways and corresponding enriched shared DEGs. Grey circles indicate enriched pathways; blue rectangles indicate down-regulated genes, and red rectangles indicate up-regulated genes. F: A pathway-gene subnetwork centered on CD36 identified using the degree method in Cytoscape software. Node colors gradually transitioned from yellow to red corresponding to ascending degree score. DEGs: Differentially expressed genes; POP: Pelvic organ prolapse; GO: Gene Ontology; KEGG: Kyoto Encyclopedia of Genes and Genomes database.

2.5 GSEA and ssGSEA analysis

The GSEA results further manifested that adipose-relevant pathways were activated in the uterosacral ligaments of recurrent POP women compared to primary POP or control women (Supplementary Figure 1A and 1B, https://doi.org/10.57760/sciencedb.xbyxb.00021). Noticeably, the “PPAR signaling pathway” was one of the most significantly motivated pathways with the highest NES score in both contrast matrices. Furthermore, some inflammatory pathways were also activated, such as “cytokine-cytokine receptor interaction” was motivated in both contrast matrices (Supplementary Figure 1A − 1D, https://doi. org/10.57760/sciencedb. xbyxb. 00021); “Toll-like receptor signaling pathway” and “NOD-like receptor signaling pathway” were activated in recurrent POP vs primary POP uterosacral ligaments (Supplementary

Figure 1A, https://doi.org/10.57760/sciencedb.xbyxb.00021); "complement and coagulation cascades" were triggered in recurrent POP vs non-POP uterosacral ligaments (Supplementary Figure 1B, https://doi.org/10.57760/sciencedb.xbyxb.00021). Nevertheless, "regulation of actin cytoskeleton" and "arrhythmogenic right ventricular cardiomyopathy" pathways were inhibited in both contrast matrices (Supplementary Figure 1A−1D, https://doi.org/10.57760/sciencedb.xbyxb.00021), and we supposed it might, to some extent, reflect a deficiency of muscle quantity or contraction in uterosacral ligaments from recurrent POP women.

The results for ssGSEA also indicated that differentially enriched pathways, including adipose-relevant pathways, could distinguish recurrent POP uterosacral ligaments apart from recurrent POP (Supplementary Figure 1E, https://doi.org/10.57760/sciencedb.xbyxb.00021) and non-POP uterosacral ligaments (Supplementary Figure 1F, https://doi.org/10.57760/sciencedb.xbyxb.00021). Moreover, the "PPAR singling pathway" was significantly positively correlated with several adipose-relevant pathways, such as "adipocytokine signaling pathway" and "fatty acid metabolism" in theses uterosacral ligaments (Supplementary Figure 1G, https://doi.org/10.57760/sciencedb.xbyxb.00021).

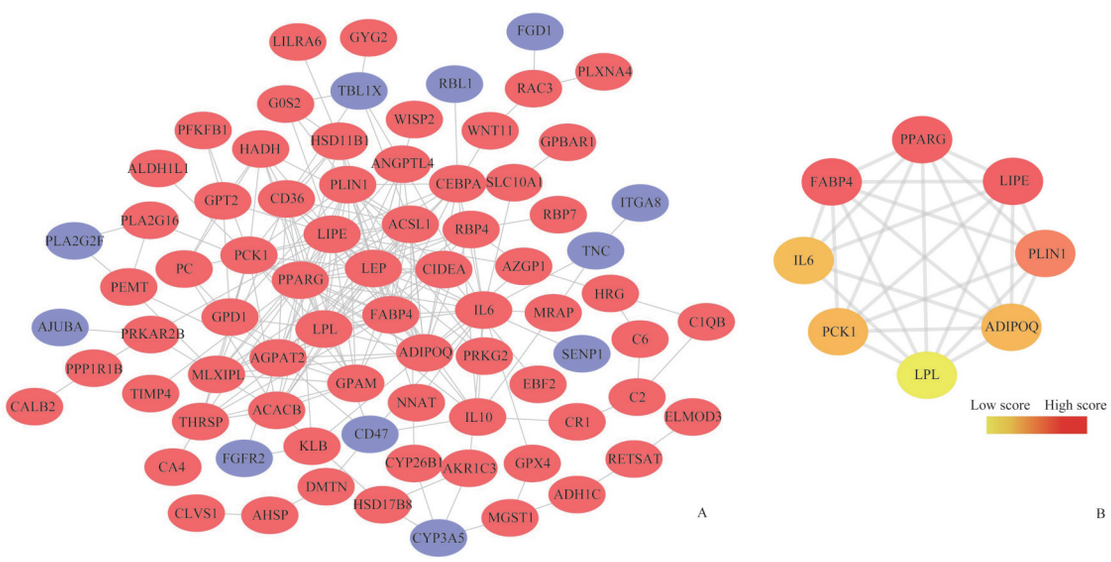

Figure 4 PPI network construction and identification of hub nodes

A: PPI network is constructed by shared DEGs between recurrent POP and primary POP uterosacral ligaments or recurrent POP and non-POP uterosacral ligaments. The red nodes represents upregulated genes, and the blue nodes represents downregulated genes. B: Eight core DEGs are identified from the PPI network using the MCODE plugin in Cytoscape software. The nodes color changes gradually from yellow to red in ascending order depending on the MCODE score. PPI: Protein-protein interaction; DEGs: Differentially expressed genes; POP: Pelvic organ prolapse.

2.6 Uterosacral ligaments microenvironment analysis

To investigate the cell composition of the microenvironment in uterosacral ligaments, we employed the xCell method to calculate the enrichment score of certain cell types in each sample. The results indicated that the enrichment score of adipocytes, monocytes, and neutrophils was significantly higher in recurrent POP uterosacral ligaments compared to non-POP and primary-POP uterosacral ligaments (Supplementary Figure 2A, https://doi.org/10.57760/sciencedb.xbyxb.00021). And the enrichment of adipocytes in recurrent POP uterosacral ligaments reached the highest score among all analyzed cell types, showing a significantly positive-correlation with the enrichment of monocytes and neutrophils (Supplementary Figure 2B, https://doi.org/10.57760/sciencedb. xbyxb. 00021). These might indicate increment of adipocytes attracted by the infiltration of

inflammatory cells into POP uterosacral ligaments. Additionally, fibroblasts and smooth muscle cells appeared to be more abundant in non-POP and primary-POP uterosacral ligaments than in recurrent POP uterosacral ligaments, nonetheless with a $P>0.05$ (Supplementary Figure 2A, https://doi.org/10.57760/sciencedb.xbyxb.00021).

The correlation analysis revealed that most hub genes showed positive associations with the enrichment of adipocyte cells in uterosacral ligaments (except *ADIPOQ*, $P>0.05$), and the enrichment of neutrophils (except *IL-6*, $P>0.05$). Notably, all 9 hub genes were significantly and positively-correlated mainly with the enrichment of monocytes in uterosacral ligaments (Supplementary Figure 2C, https://doi.org/10.57760/sciencedb.xbyxb.00021). Given that most of the 9 hub genes were enriched in the PPAR signaling pathway, we further analyzed the relationship of the PPAR signaling pathway and the cell composition of the microenvironment in uterosacral ligaments. The results also revealed the PPAR signaling pathway positively associated with the enrichment of adipocytes, preadipocytes, monocytes, and neutrophils, while negatively associated with smooth muscles and fibroblasts (Supplementary Figure 2D, https://doi.org/10.57760/sciencedb.xbyxb.00021).

2.7 Significant adipose accumulation in the uterosacral ligaments of an ovariectomized SVD rat model

On day 21 after modeling, the estrogen levels of rats in the ovariectomized SVD group were significantly lower than those in the sham and non-ovariectomized SVD groups (Figure 5A). Meanwhile, the urodynamic results showed that BLPP values were higher in the ovariectomized SVD group than in the non-ovariectomized SVD group, whose values were higher than those of the sham group, whereas MBC and ALPP were not significantly changed in the 3 groups (Figure 5B). In addition, the results of Masson staining showed that there was significant adipose accumulation and reduction of muscle fibers and collagen fibers in the uterosacral ligaments of rats in the ovariectomized SVD group compared with rats in the sham and non-ovariectomized SVD groups (Figure 5C). Real-time RT-PCR results also verified that the hub genes, *ADIPOQ, IL-6, PCK1,* and *PLIN1* were all significantly highly expressed in the uterosacral ligament of ovariectomized SVD rats (Figure 5D).

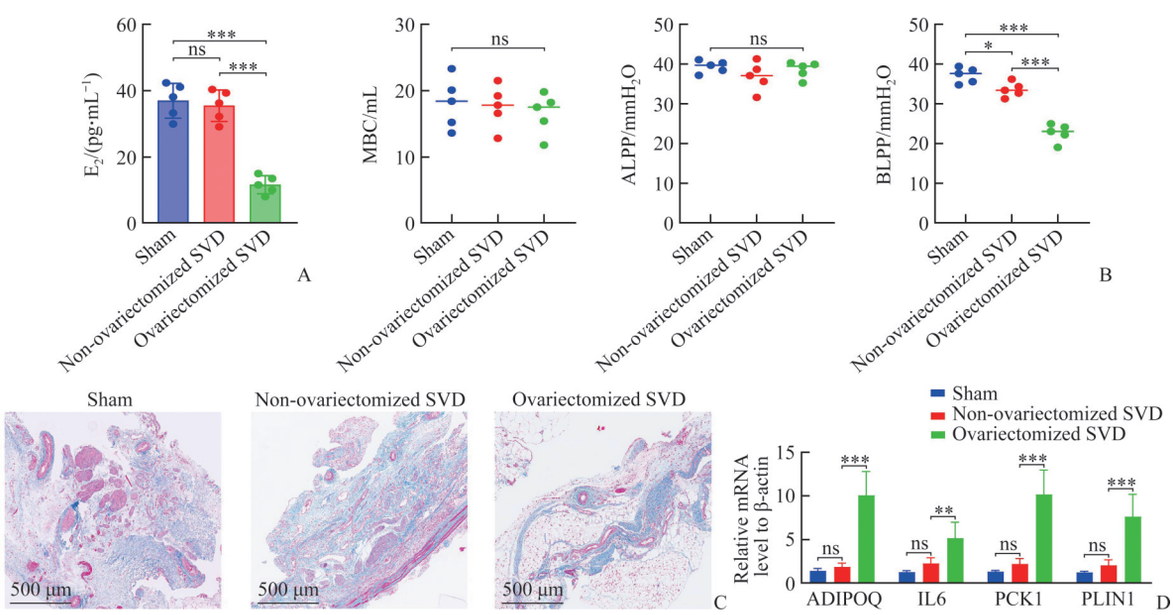

Figure 5 Significant adipose accumulation in the uterosacral ligaments of the ovariectomized SVD rat model

A: Detection of blood estrogen levels in each group of rats were measured by ELISA. B: Urodynamics showed the MBC, BLPP, ALPP values in each group of rats. C: Histological changes in the uterosacral ligaments of rats in each group were detected by the Masson staining. D: Expression of hub genes in the uterosacral ligaments of rats in each group was examined by real-time RT-PCR. *$P<0.05$, **$P<0.01$, ***$P<0.001$; ns: Not significant. E_2: Estradiol; MBC: Maximum bladder capacity; BLPP: Bladder leak-point pressure; ALPP: Abdominal leak point pressure; SVD: Simulated vaginal delivery.

3 Discussion

Uterosacral ligaments are assumed as visceral ligaments with mesentery-like components, such as vessels, nerves, fibers, muscle tissues, and adipose tissues, and uterosacral ligament suspension has become a common procedure in the surgical treatment of POP[10]. By applying a novel histologic quantification system, Orlicky, et al[22] classified POP uterosacral ligaments into 3 histologic phenotypes: 1) Uterosacral ligaments with elevated adipose accumulation (POP-A); 2) uterosacral ligaments with enhanced inflammation (POP-I); and 3) uterosacral ligaments with aberrant vasculature (POP-V). Interestingly, they found that both POP-A and POP-I phenotypes exhibited significantly higher adipose tissue deposition, combinecl with smooth muscle fiber loss in uterosacral ligaments. Moreover, adipose content showed a significantly positive correlation with parity (number of vaginal deliveries, $P<0.05$), while no significant association was observed with body mass index of patients ($P>0.05$).

Consistently, our bioinformatic analysis indicated that the enrichment of adipocytes of uterosacral ligaments in recurrent POP was even higher than that in primary POP, while the enrichment of fibroblasts and smooth muscle cells seem to be even lower. Besides, our in vivo experiments showed that ovariectomized SVD rats developed significant urodynamic changes similar to stress urinary incontinence, as well as obvious adipose accumulation in the uterosacral ligament. Hence, we could hypothesize that metabolic changes due to declining estrogen and mechanical damage from repeated deliveries lead to hypertrophy of the uterosacral ligaments[23-24]. Furthermore, the adipose accumulation would potentially induce an inflammatory circumstance by a variety of intrinsic signals, such as adipokines secretion, adipocyte death, hypoxia, and mechanical stress[25]. In return, a local dysregulated proinflammatory state would aggravate the accumulation of fat in surrounding adipose tissues[26].

Although macrophages did not differ among recurrent POP, primary POP, and non-POP uterosacral ligaments in our results, both monocytes and neutrophils were significantly enriched in recurrent POP uterosacral ligaments when compared to non-POP or primary-POP uterosacral ligaments. Neutrophils were reported to be the initial immune cells to infiltrate adipose tissues, and their activation would release inflammatory factors to recruit macrophages and other immune cells[27]. As a well-known pro-inflammatory adipokine, leptin (encoded by *LEP*) induced endothelial cell activation thereby recruiting monocytes from circulating blood to adipose tissues[28]. Moreover, we found that classic inflammatory cytokine, IL-6, was elevated in the uterosacral ligament of recurrent POP and was positively associated with the enrichment of adipocytes and monocytes. In addition to immune cells, adipocytes can also secrete IL-6, which promoted adipose tissue-associated macrophage infiltration and pro-inflammatory responses, acting in contrast to the role of muscle-secreted IL-6 in a certain physiological context[29].

We found that the PPAR signaling pathway, which plays a modulating role in both lipid and glucose homeostasis, was significantly activated in the recurrent POP uterosacral ligaments. The PPARs are essential transcript factors located in the cell nucleus and important for lipid metabolism, including the isoforms PPAR-α, PPAR-β/δ, and PPAR-γ[30]. Notably, PPAR-γ is reported to be predominantly expressed in adipose tissue and serves as a master regulator of adipogenesis and adipocyte differentiation[31]. The expression of PPAR-γ was elevated in adipose tissues in obesity, and the adipose-specific deletion of PPAR-γ resulted in the failure of adipose tissue development in mice[32]. Our results showed that PPAR-γ and its downstream target genes (also in the hub DEGs), such as *PCK1, ADIPOQ, PLIN1, FABP4, CD36,* were increased in recurrent POP uterosacral ligaments. The *ADIPOQ* gene is highly and specifically expressed in adipose tissues, and encodes the peptide hormone adiponectin, which could promote 3T3-L1 fibroblasts to differentiate more rapidly into adipocytes and exhibit a more persistent and more robust gene expression for PPAR-γ[33].

The class B scavenger receptor and fatty acid transporter, CD36, has been defined as a marker for adipocyte progenitor cells for its facilitation in lipid uptake and accumulation in adipose tissue-derived stem cells with a strong predisposition for adipocyte differentiation[34]. Other study[35] has reported that FABP4 and PPAR-γ activate each other to form a feedback loop that critically controls the second phase of

adipogenesis. Overexpression of PCK1 in mice could induce adipocyte enlargement and thus fat accumulation by increasing glycerogenesis, fatty acid esterification, and triglyceride synthesis[36]. The gene *PLIN1* encodes Perilipin 1, an enzyme with capabilities for encapsulating lipid droplets inside adipocytes to protect them from enzymatic degradation[37]. Lipid droplet growth and differentiation were inhibited in adipose stromal-vascular cells from PLIN1 null (−/−) mice, which would be rescued by PLIN1 overexpression or enhanced PPAR-γ stimulation[38]. Therefore, the activation of the PPAR signaling pathway would contribute to an increased adipose and inflammatory state in uterosacral ligaments from women suffering recurrent POP.

Despite the above considerations, there are some limitations to our analysis. Firstly, the sample size for control or POP tissues was small due to the availability of information, thus expanding the sample size would make the current results stronger. Secondly, because the clinical information provided in the GSE28660 was limited, some bias factors could not be excluded, such as the body mass index of patients. Thirdly, because the incidence of recurrent POP and surgical indications vary in different medical regions, samples of the uterosacral ligament from patients with recurrent POP are not easy to be collected locally, and therefore we only performed bioinformatics analysis at the transcriptome level and animal experiments for validation. In the future, it may be necessary to include more relevant clinical samples for Western blotting and immunohistochemistry assays to further confirm our conclusions.

In conclusion, our analysis approach provides a transcriptomic perspective to explain molecular changes in recurrent POP uterosacral ligaments when compared to primary POP or non-POP uterosacral ligaments. Both, activated adipose- and inflammation-relevant pathways and genes are upregulated in recurrent POP uterosacral ligaments, which might indicate increased adipose accumulation, further accompanying inflammation in uterosacral ligaments, and thus contributing to the development of recurrent POP in postmenopausal women.

Contribution: ZHOU Yanhua and YAN Dayu Acquired and analyzed data, drafted the manuscript; ZHANG Xiulan Helped interpret data and prepared figures and tables; LI Xuhong and YAN Wenguang Revised the manuscript; JIANG Li Conceived and designed the study, acquired and analyzed data, revised the manuscript. The final version of the manuscript has been approved and read by all authors.

Conflict of interest: The authors declare that they have no conflicts of interest to disclose.

References

[1] Raju R, Linder BJ. Evaluation and management of pelvic organ prolapse[J]. Mayo Clin Proc, 2021, 96(12): 3122-3129. https://doi.org/10.1016/j.mayocp.2021.09.005.

[2] Wu JM, Matthews CA, Conover MM, et al. Lifetime risk of stress urinary incontinence or pelvic organ prolapse surgery[J]. Obstet Gynecol, 2014, 123(6): 1201-1206. https://doi. org/10.1097/AOG.0000000000000286.

[3] Schulten SFM, Claas-Quax MJ, Weemhoff M, et al. Risk factors for primary pelvic organ prolapse and prolapse recurrence: an updated systematic review and meta-analysis[J]. Am J Obstet Gynecol, 2022, 227(2): 192-208. https://doi.org/10.1016/j.ajog.2022.04.046.

[4] St Martin B, Markowitz MA, Myers ER, et al. Estimated national cost of pelvic organ prolapse surgery in the United States[J]. Obstet Gynecol, 2024, 143(3): 419-427. https://doi.org/10.1097/AOG.0000000000005485.

[5] Ismail S, Duckett J, Rizk D, et al. Recurrent pelvic organ prolapse: International Urogynecological Association Research and Development Committee opinion[J]. Int Urogynecol J, 2016, 27(11): 1619-1632. https://doi.org/10.1007/s00192-016-3076-7.

[6] Geoffrion R, Larouche M. Guideline No. 413: surgical management of apical pelvic organ prolapse in women[J/OL]. J Obstet Gynaecol Can, 2021, 43(4): 511-523. e1[2024-06-28]. https://doi.org/10.1016/j.jogc.2021.02.001.

[7] Hill AM, Pauls RN, Crisp CC. Addressing apical support during hysterectomy for prolapse: a NSQIP review[J]. Int Urogynecol J, 2020, 31(7): 1349-1355. https://doi.org/10.1007/s00192-020-04281-w.

[8] Kieserman-Shmokler C, Swenson CW, Chen LY, et al. From molecular to macro: the key role of the apical ligaments in uterovaginal support[J]. Am J Obstet Gynecol, 2020, 222(5): 427-436. https://doi.org/10.1016/j.ajog.2019.10.006.

[9] Donaldson K, Huntington A, De Vita R. Mechanics of uterosacral ligaments: current knowledge, existing gaps, and future directions[J]. Ann Biomed Eng, 2021, 49(8): 1788-1804. https://doi.org/10.1007/s10439-021-02755-6.

[10] Cola A, Marino G, Milani R, et al. Native-tissue prolapse repair: Efficacy and adverse effects of uterosacral ligaments suspension at 10-year follow up[J]. Int J Gynaecol Obstet, 2022, 159(1): 97-102. https://doi.org/10.1002/ijgo.14096.

[11] Li XJ, Pan HT, Chen JJ, et al. Proteomics of uterosacral ligament connective tissue from women with and without pelvic organ prolapse[J/OL]. Proteomics Clin Appl, 2019, 13(4): e1800086[2024-06-11]. https://doi.org/10.1002/prca.201800086.

[12] Liu X, Su M, Wei L, et al. Single-cell analysis of uterosacral ligament revealed cellular heterogeneity in women with pelvic organ prolapse[J]. Commun Biol, 2024, 7(1): 159. https://doi.org/10.1038/s42003-024-05808-3.

[13] Ritchie ME, Phipson B, Wu D, et al. Limma powers differential expression analyses for RNA-sequencing and microarray studies[J/OL]. Nucleic Acids Res, 2015, 43(7): e47 [2023-07-12]. https://doi.org/10.1093/nar/gkv007.

[14] The Gene Ontology Consortium. The Gene Ontology Resource: 20 years and still GOing strong[J]. Nucleic Acids Res, 2019, 47 (D1): D330-D338. https://doi.org/10.1093/nar/gky1055.

[15] Kanehisa M, Furumichi M, Sato Y, et al. KEGG: integrating viruses and cellular organisms[J]. Nucleic Acids Res, 2021, 49 (D1): D545-D551. https://doi.org/10.1093/nar/gkaa970.

[16] Geistlinger L, Csaba G, Santarelli M, et al. Toward a gold standard for benchmarking gene set enrichment analysis[J]. Brief Bioinform, 2021, 22(1): 545-556. https://doi.org/10.1093/bib/bbz158.

[17] Hänzelmann S, Castelo R, Guinney J. GSVA: gene set variation analysis for microarray and RNA-seq data[J]. BMC Bioinformatics, 2013, 14: 7. https://doi.org/10.1186/1471-2105-14-7.

[18] Aran D, Hu Z, Butte AJ. xCell: digitally portraying the tissue cellular heterogeneity landscape[J]. Genome Biol, 2017, 18(1): 220. https://doi.org/10.1186/s13059-017-1349-1.

[19] Guo T, Du Z, Wang XQ, et al. Ovariectomy with simulated vaginal delivery to establish a rat model for pelvic organ prolapse[J]. Connect Tissue Res, 2023, 64(4): 376-388. https://doi.org/10.1080/03008207.2023.2199091.

[20] Liu Z, Tang Y, Liu J, et al. Platelet-rich plasma promotes restoration of the anterior vaginal wall for the treatment of pelvic floor dysfunction in rats[J]. J Minim Invasive Gynecol, 2023, 30(1): 45-51. https://doi.org/10.1016/j.jmig.2022.10.004.

[21] Gong J, Gong H, Liu Y, et al. Calcipotriol attenuates liver fibrosis through the inhibition of vitamin D receptor-mediated NF-κB signaling pathway[J]. Bioengineered, 2022, 13(2): 2658-2672. https://doi.org/10.1080/21655979.2021.2024385.

[22] Orlicky DJ, Guess MK, Bales ES, et al. Using the novel pelvic organ prolapse histologic quantification system to identify phenotypes in uterosacral ligaments in women with pelvic organ prolapse[J/OL]. Am J Obstet Gynecol, 2021, 224(1): 67.e1-e18[2024-07-11]. https://doi.org/10.1016/j.ajog.2020.10.040.

[23] Reddy RA, Cortessis V, Dancz C, et al. Role of sex steroid hormones in pelvic organ prolapse[J]. Menopause, 2020, 27(8): 941-951. https://doi.org/10.1097/GME.0000000000001546.

[24] Cattani L, Decoene J, Page AS, et al. Pregnancy, labour and delivery as risk factors for pelvic organ prolapse: a systematic review[J]. Int Urogynecol J, 2021, 32(7): 1623-1631. https://doi.org/10.1007/s00192-021-04724-y.

[25] Liu R, Nikolajczyk BS. Tissue immune cells fuel obesity-associated inflammation in adipose tissue and beyond[J]. Front Immunol, 2019, 10: 1587. https://doi.org/10.3389/fimmu.2019.01587.

[26] Kawai T, Autieri MV, Scalia R. Adipose tissue inflammation and metabolic dysfunction in obesity[J]. Am J Physiol Cell Physiol, 2021, 320(3): C375-C391. https://doi.org/10.1152/ajpcell.00379.2020.

[27] Uribe-Querol E, Rosales C. Neutrophils actively contribute to obesity-associated inflammation and pathological complications[J]. Cells, 2022, 11(12): 1883. https://doi.org/10.3390/cells11121883.

[28] Martínez-Sánchez N. There and back again: leptin actions in white adipose tissue[J]. Int J Mol Sci, 2020, 21(17): 6039. https://doi.org/10.3390/ijms21176039.

[29] Han MS, White A, Perry RJ, et al. Regulation of adipose tissue inflammation by interleukin 6[J]. Proc Natl Acad Sci USA, 2020, 117(6): 2751-2760. https://doi.org/10.1073/pnas.1920004117.

[30] Montaigne D, Butruille L, Staels B. PPAR control of metabolism and cardiovascular functions[J]. Nat Rev Cardiol, 2021, 18(12): 809-823. https://doi.org/10.1038/s41569-021-00569-6.

[31] Wang S, Lin YK, Gao L, et al. PPAR-γ integrates obesity and adipocyte clock through epigenetic regulation of *Bmal1*[J]. Theranostics, 2022, 12(4): 1589-1606. https://doi.org/10.7150/thno.69054.

[32] Jones JR, Barrick C, Kim KA, et al. Deletion of PPARgamma in adipose tissues of mice protects against high fat diet-induced obesity and insulin resistance[J]. Proc Natl Acad Sci USA, 2005, 102(17): 6207-6212. https://doi.org/10.1073/pnas.0306743102.

[33] Yang W, Yang C, Luo J, et al. Adiponectin promotes preadipocyte differentiation via the PPARγ pathway[J]. Mol Med Rep, 2018, 17(1): 428-435. https://doi.org/10.3892/mmr.2017.7881.

[34] Gao H, Volat F, Sandhow L, et al. CD36 is a marker of human adipocyte progenitors with pronounced adipogenic and triglyceride accumulation potential[J]. Stem Cells, 2017, 35(7): 1799-1814. https://doi.org/10.1002/stem.2635.

[35] Berger E, Géloën A. FABP4 controls fat mass expandability (adipocyte size and number) through inhibition of CD36/SR-B2 signalling[J]. Int J Mol Sci, 2023, 24(2): 1032. https://doi.org/10.3390/ijms24021032.

[36] Li Q, Spalding KL. The regulation of adipocyte growth in white adipose tissue[J]. Front Cell Dev Biol, 2022, 10: 1003219. https://doi.org/10.3389/fcell.2022.1003219.

[37] Desgrouas C, Thalheim T, Cerino M, et al. Perilipin 1: a systematic review on its functions on lipid metabolism and atherosclerosis in mice and humans[J]. Cardiovasc Res, 2024, 120(3): 237-248. https://doi.org/10.1093/cvr/cvae005.

[38] Lyu Y, Su X, Deng J, et al. Defective differentiation of adipose precursor cells from lipodystrophic mice lacking perilipin 1 [J/OL]. PLoS One, 2015, 10(2): e0117536[2024-07-05]. https://doi.org/10.1371/journal.pone.0117536.

(Edited by PENG Minning)

本文引用：周艳华, 严大宇, 张秀兰, 李旭红, 严文广, 姜丽. 转录组学分析揭示复发性盆腔器官脱垂的绝经后妇女存在子宫骶韧带“脂肪化”[J]. 中南大学学报(医学版), 2024, 49(11): 1808-1820. DOI:10.11817/j.issn.1672-7347.2024.230308

Cite this article as: ZHOU Yanhua, YAN Dayu, ZHANG Xiulan, LI Xuhong, YAN Wenguang, JIANG Li. Transcriptomic analysis reveals “adipogenesis” in the uterosacral ligaments of postmenopausal women with recurrent pelvic organ prolapse[J]. Journal of Central South University. Medical Science, 2024, 49 (11): 1808-1820. DOI:10.11817/j.issn.1672-7347.2024.230308